

# On the $1/f$ Noise and Non-Integer Harmonic Decay of the Interaction of a Finger Sliding on Flat and Sinusoidal Surfaces

Michaël Wiertlewski\*

CEA, LIST,  
Sensory and Ambient Interfaces Laboratory,  
18 route du Panorama, BP6, 92295  
Fontenay-Aux-Roses, France

Charles Hudin†

CEA, LIST,  
Sensory and Ambient Interfaces Laboratory,  
18 route du Panorama, BP6, 92295  
Fontenay-Aux-Roses, France

Vincent Hayward‡

UPMC Univ Paris 06,  
UMR 7222, Institut des Systèmes  
Intelligents et de Robotique,  
F-75005, Paris, France

## ABSTRACT

Fluctuations of the frictional force arising from the stroke of a finger against flat and sinusoidal surfaces are studied. A custom-made high-resolution friction force sensor, able to resolve milli-newton forces, was used to record those fluctuations as well as the net, low-frequency components of the interaction force. Measurements show that the fluctuations of the sliding force are highly non-stationary. Despite their randomness, force spectra averages reveal regularities. With a smooth, flat, but not mirror-finish, surface the background noise follows a  $1/f$  trend. Recordings made with pure-tone sinusoidal gratings reveal complexities in the interaction between a finger and a surface. The fundamental frequency is driven by the periodicity of the gratings and harmonics follow a non-integer power-law decay that suggests strong nonlinearities in the fingertip interaction. The results are consistent with the existence of a multiplicity of simultaneous and rapid stick-slip relaxation oscillations. Results have implications for high fidelity haptic rendering and biotribology.

**Index Terms:** H.5.2 [Information Interfaces and Presentation]: User Interface—Haptic I/O; H.5.1 [Multimedia Information Systems]: Audio input/output; H.1.2 [Information Systems]: User/Machine Systems—Human information processing; I.3.7 [Computer Graphics]: Three-Dimensional Graphics and Realism. Virtual Reality

## 1 INTRODUCTION

When sliding on most surfaces, human fingers generate audible noise. If the surface in question is able to acoustically radiate—as in the case of the sounding board of a guitar—the noise can actually be quite loud, denoting that a significant portion of the work done during sliding is transformed into acoustic energy which is dissipated in part in the tissues and in the solid object. Although originating from the skin it has recently been found that these vibrations can propagate far, and over a wide frequency range, in the tissues of the arm [8]. The reader can easily verify that such noise is generated even when sliding a finger on the mirror finish of a glass surface, unless the contact is lubricated.

Since the early works of Katz [13], as well as with more recent studies [11, 12, 10, 20, 3], it is generally accepted that these vibrations play a determinant role in the perception of textures, or absence thereof. One factor behind the generation of the oscillations by the sliding skin is the distribution and nature of asperities on surfaces which result from erosion, wear, manufacturing, or growth of the material. Another factor is the nature of the material (or fabric)

\*e-mail: michael.wiertlewski@cea.fr

†e-mail: charles.hudin@cea.fr

‡e-mail: hayward@isir.upmc.fr

of which the surface is made, since two surfaces having the same geometry can create very different acoustic signatures. The finger also contributes peculiar geometrical and material properties that determine the tribology of the contact [1, 21].

The motivation for our research is in the area of haptic virtual reality and computer simulations, where tactual texture plays an important role in realism [22, 5, 6]. Interestingly, the synthesis of rich, artificial tactual textures have tended to resemble audio rendering techniques, being based on generating a spatial waveform that is played at the speed of exploration [22]. The artificial waveform can be created either from measurements [9], or procedurally from stochastic or fractal models [19, 7]. All these synthesis processes are based on the assumption that the contact is made by a rigid probe that obeys an elastic linear law, and on simplified solid friction models to generate stimuli. As previously presented, these assumptions break down completely in the case of a bare finger [25].

Almost no work has been dedicated to this analysis of the dynamics of finger-surface interactions during steady sliding, with the perspective of simulating it. The fingertip exhibits non trivial friction phenomena that are not well understood [1], yet even under the assumption of linear elasticity, the frictional properties of soft material with rigid, rough surfaces are not trivial to model [18]. The output of a measurement depends on many parameters such as the viscoelasticity and the non-linearity of the finger and the skin [17, 16, 23]. The friction force itself varies according to various conditions including normal loading and hydration of the skin [24, 2].

In the present study, we asked whether the vibrations generated during the slip of a finger on smooth and sinusoidal surfaces could be characterized in terms of their spatial spectrum content. In other words, we wondered whether these vibrations presented characteristics of invariance or regularities with respect to the applied force and the slip velocity, that is to say, whether these vibrations encode the underlying surface geometry.

Employing a specially engineered sensor [26], we recorded the force *fluctuations* of a finger sliding on accurately manufactured flat surfaces and sinusoidal gratings. This sensor can resolve sub milli-newton forces with a high dynamic range. We then performed a spectral analysis of the tangential force component in the spatial domain and sought to discover invariants. The analysis of the spatial frequency content of these vibrations gave some insights into the mechanisms that can possibly be at play.

The friction force signal can be represented by the superposition of two contributions. One being a background noise that follows a  $1/f$  relationship, and the second being, on average only, a harmonic expansion of the original frequency that decays according to a non integer power-law, suggesting a relaxation oscillatory process. Results have implications for the synthesis of artificial tactile stimuli and in the field of biotribology.

## 2 CHOICE OF SURFACES

The motivation for the choice of sinusoidal profiles was not that they represent “pure tones” in the spectral domain, but rather that

they provide a smooth change of curvature within the contact regions with the skin. In effect, in the range of amplitudes, periods and interaction force magnitudes that we studied, a finger is not guaranteed to interact through one single connected region and can possibly touch only at the apices of the individual ridges. We did not control for this possibility, but from a general perspective, such occurrences are part of the normal tactual exploration process and were left intact. In any case, sinusoidal profiles guaranteed that the curvature varied smoothly within restricted intervals.

Other profiles that were considered include triangular and square profiles, all having first-order discontinuities to which the skin would be exposed. For the purposes of the present study, discontinuities have the grave inconvenience that sharp edges translate into undefined (infinite) local strains. Physically, undefined strains correspond to damage, a type of interaction which can include abrasion, delamination and other effects, and which are interactions that are normally avoided during tactual slip.

In the choice and manufacturing of the surfaces, we also considered the question of length scales, which is central to the concept of roughness. An undulating or a flat surface is compatible with the presence of irregularities at length scales that are 2 or 3 orders of magnitude smaller than the main textural components, the so-called 'surface finish' in plain language. Even if, due to the St Venant's principle, small-scale asperities are of no mechanical consequences a few microns inside the skin during static touch, such is not the case during sliding because their presence or absence has impact on skin tribology. There is a variety of phenomena at play including the possible presence of trapped foreign bodies and liquids that modify tribology according to the nature of small-scale asperities.

Healthy fingers permanently exude sweat and the *stratum corneum*, specifically, is a highly hydrophilic milieu. The presence of small-scale asperities, in contrast to amorphous glassy finishes, have impact on skin keratin plasticization and on the behavior of interfacial water, modifying adhesion [1].

### 3 FINGER-SURFACE INTERACTION MEASUREMENT

From the above considerations, to approach the question of the vibrations induced by sliding, we performed highly accurate measurements of the tangential force component of the interaction force, that due to friction, during steady sliding of the finger on flat and undulating sinusoidal surfaces with controlled surface finishes.

The apparatus comprised a finger position measurement device, a specifically designed friction force transducer, and a conventional six-axis force sensor for a complete characterization of low frequency interaction force components.

#### 3.1 Hardware Components

The three hardware components measured three different aspects of the interaction, namely: the position of the finger, the friction force fluctuations, and the net normal and tangential forces. Sliding velocity was estimated from suitably processed differentiation of the position signal. Fig.1 shows a picture of the apparatus during a measurement.

The main component is a custom-made piezoelectric sensor that operates in the direction tangential to the scanned surface in the 2.5–350 Hz frequency range and with a sensitivity of 13 N/V. The sensor was engineered to perform with noise floor of 50  $\mu$ N. The friction-force fluctuation transducer was built around a disk multilayer piezo bender, A, (CMBR07, Noliac Group A/S, Kvistgaard, Denmark) that converted the tangential load force into electrical charges. The piezoelectric sensor acted as a voltage generator coupled in series with a capacitor. The voltage was conditioned by an instrumentation amplifier (LT1789, Linear Technology Corp., Milpitas, CA, USA). Two resistances passed the generated charges to the ground and therefore create a high-pass filter. The value of the

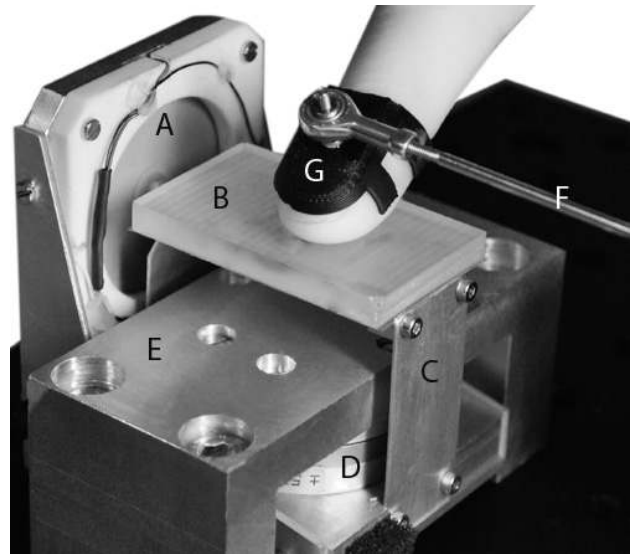


Figure 1: Measurement Bench. The texture is double-sided taped to the piezoelectric force transducer that measures frictional force arising from the finger sliding on it. The finger is located by a LVDT fixed to the finger through a universal joint.

resistances were chosen to produce a first-order, high-pass filter response with a 2.5 Hz cutoff frequency.

The interchangeable gratings, B, were bonded to a plate with double sided tape. The plate was suspended between two leaf springs, C, connected to the hollow center of the piezoelectric bender with a flexural joint that was very stiff in the axial direction. The resulting stiffness was  $8.0 \times 10^4$  N/m, which is two orders of magnitude stiffer than a finger [16]. Hence, it provides a non-ambiguous measurement of the tangential sliding force. The suspended mass was estimated to be 12 g and therefore the natural frequency of the sensor was at 410 Hz. Figure 2 shows the response of the sensor derived from its impulse response.

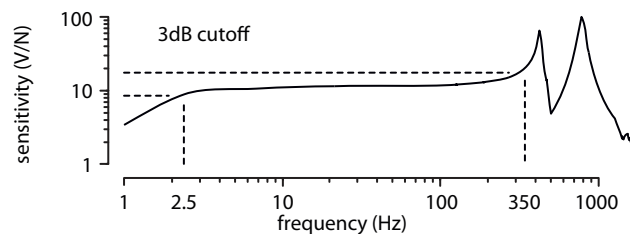


Figure 2: Sensitivity of the sensor as a function of frequency from its impulse response. The flat band is the range 2.5 Hz to 350 Hz.

The second element of the apparatus was a conventional strain gauge force sensor, D, (Mini 40, ATI Industrial Automation, Apex, NC, USA) which responded to the low frequency force components along the normal and tangential directions. It was placed underneath the piezoelectric transducer on the load path to the mechanical ground, E. In order to maximize bandwidth, the mechanical arrangement, see Fig. 1, minimized the distance between the point of application of finger interaction force and the sensor flanges by mounting it 'upside-down'. The resolution was about 50 mN.

The subject's finger was located by a LVDT transducer (SX 12N060, Sensorex SA, Saint-Julien-en-Genevois, France) that could resolve 3  $\mu$ m on a 40 mm stroke. Prior calibration was performed using precision micro-stage. The finger was rigidly linked to the

movable core of the linear transducer, F, by a clip mounted on the nail side of the finger via a joint, G, totaling 5 degrees of freedom. The alignment of the LVDT was provided by adjustable linear stages.

Analog signals were acquired by a 16-bit data acquisition board (PCI-6229, National Instruments Corp., Austin, TX, USA) hosted by standard microcomputer. The sampling period was set at 10 kHz in order to have a comfortable sampling margin and reduce distortion during post-filtering.

### 3.2 Digital signal processing

The raw data were sampled in the temporal domain and therefore depended on the sliding velocity. In order to express the data with the velocity as a parameter, it had to be resampled in the spatial domain using a fixed spatial sampling period. The data retrieved from the measurement of a finger sliding on a given texture, Fig. 3a, were interpolated at each multiple of the discrete position steps obtained from the position trajectory as in Fig. 3b. The steady slip region was cropped out by truncating the initial transitory period of the recordings such that the samples were kept in the range  $5 \text{ mm} < x_c < 35 \text{ mm}$ . The interpolation-resampling procedure was applied to the tangential force measurements,  $f_T$ , from the piezoelectric transducer and to the normal and the tangential forces measured from the strain-gauge sensor.

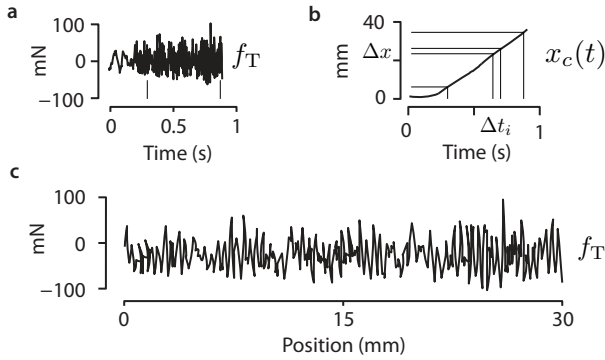


Figure 3: Resampling procedure. (a) Raw position data. (b) Raw force data. (c) Resampled force as a function of position.

The force frequency components above 350 Hz were filtered out of the measurements by performing a fast Fourier transform on the signal, truncating the spectrum and then reconstructing the signal using the inverse Fourier transform. The spectral domain processing provides a sharp cut-off, phase distortion-free signal conditioning. Velocity was computed by differentiating the position after applying a zero-phase moving average filter over 9 samples. It was then interpolated in space domain using the same procedure as above.

### 3.3 Gratings

We used sinusoidal gratings with height profiles expressed by  $h(x) = A \sin(2\pi/\lambda)$ . One profile, termed the nominal profile, had an amplitude of  $A = 25 \mu\text{m}$  and a spatial period of  $\lambda = 1.96 \text{ mm}$ . The other four had different amplitudes,  $A = 12.8$  and  $A = 50 \mu\text{m}$ , and spatial periods,  $\lambda = 1.76$  and  $2.5 \text{ mm}$ .

The gratings were cast from the exact same stainless steel gratings that were employed in the study in reference [15]. We first made silicon molds (RTV 181, Esprit Composite, Paris, France) and then duplicates were manufactured by casting epoxy resin (EP 141, Esprit Composite, Paris, France). This process can reproduce details as small as  $1 \mu\text{m}$ . Perceptually, the resulting epoxy duplicate

gratings feel as rough as their steel originals. Microscopic inspection did not reveal any surface imperfections. They were milled down to  $50 \times 30 \text{ mm}$  rectangular samples.

A flat surface was made with the same epoxy resin. The surface was rectified with a milling machine with a very low feed rate and a high speed. The resulting roughness was homogeneous with an  $R_a$  smaller than  $1 \mu\text{m}$  and the surface finish felt similar to that of the sinusoidal surfaces.

### 3.4 Participants and procedure

Two participants made the recordings. One of them was the first author. They were aged 24 and 26 and did not present scars or burn marks on their fingertips. They washed their hands before the session. They practiced the skill of maintaining the normal force and the velocity as constant as possible during recordings.

They sat in front of the apparatus such that their arms could move without resistance and recorded the sliding interaction force. Velocity and normal force were held as constant as possible during a single recording. The trials were selected according to how steady was the velocity and the normal force. Each participant made 50 satisfactory recordings with each texture. Recordings lasted less than one second, so that slowly varying effects due to viscoelastic behavior of a fingertip would not interfere with the results.

The velocity and normal force during every measurement matched standard exploratory conditions. Velocities ranged from  $14 \text{ mm/s}$  to  $339 \text{ mm/s}$  with a mean of  $127 \text{ mm/s}$ . Normal forces were in the range of  $0.14 \text{ N}$  to  $2.44 \text{ N}$  with a mean of  $0.8 \text{ N}$ .

## 4 OBSERVATIONS ON THE RESULTS

The frequency content of the measurements made on the texture reveals multiple features of the transformation between the single wave grating and the engendered force fluctuations. Each of the following section discusses a feature of the signal. The first observation is that two recordings made in similar conditions do not produce the same spectral content. Nevertheless some properties emerge from the *averages* of large numbers of trials. Signal energy decays in a  $1/f$  fashion and all harmonics are present with decreasing amplitudes according to a non-integer power law.

### 4.1 Lack of Stationarity

Even with similar interaction forces and velocities in, recordings presented great variations of amplitude and frequency content. Figure 4a,b,c shows the spectra of three measurements taken in similar conditions. In the low frequencies, the spatial spectra can have different decays and the amplitude of the fundamental changed. Its frequency is fixed, however, since it corresponds to that of the underlying surface. Harmonics are all present in most, but not all, of the recordings and their amplitudes also varied in each recording.

Averaging the spectra of many recordings, however, as shown in Fig. 4d, smooth the variations of spectra and a pattern emerges. The overall spectral content appears to be composed of two major components. The first component is a background noise that follows a  $1/f$  law. The second component is, on average only, a periodic component with fundamental and harmonics. This  $1/f$  noise and harmonics appear in the recordings in a non-predictable fashion, and not all the measurements exhibit these properties.

As one can expect, the fundamental frequency component is well represented and corresponded to the spatial frequency of the single-wave grating used. In addition to this fundamental, all harmonics appeared, suggesting the presence of strong nonlinearities in the transformation.

### 4.2 Energy Decay In Background Noise

Using recordings made with the flat surface, we further investigated the pattern of background noise. Figure 5 shows each individual

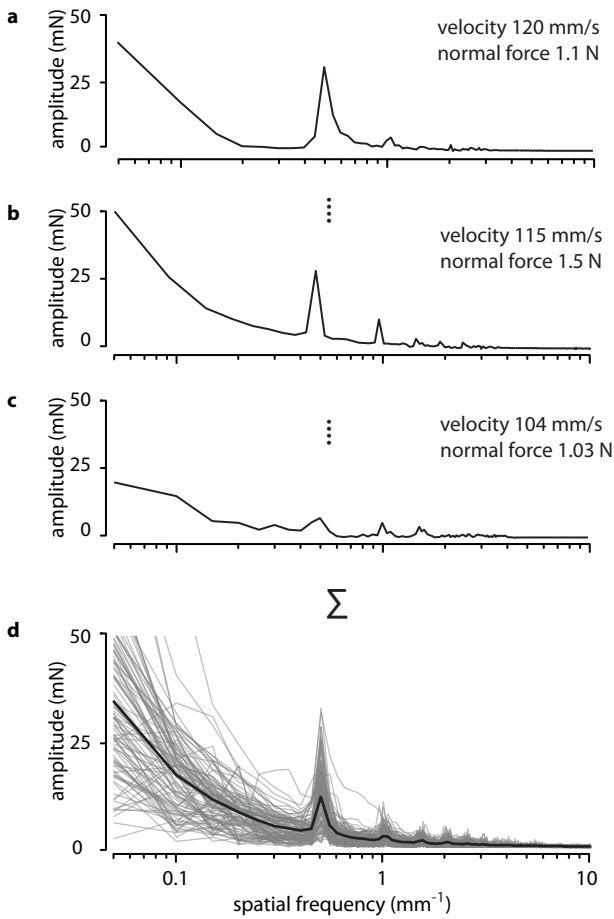


Figure 4: Three typical measurements with a finger sliding on a  $50 \mu\text{m}$  amplitude,  $1.96 \text{ mm}$  spatial period grating. One hundred measurements in grey, and their average spectrum in black.

measurement in light gray and the average spectrum in black. Furthermore, the spectrum of each individual measurement are fitted with a power function  $S(k) = \beta/k^\alpha$  with  $k = 1/\lambda$  being the spatial frequency,  $\alpha$  and  $\beta$  the fitting coefficients. The distribution of the fitted coefficients can be seen in Fig. 6.

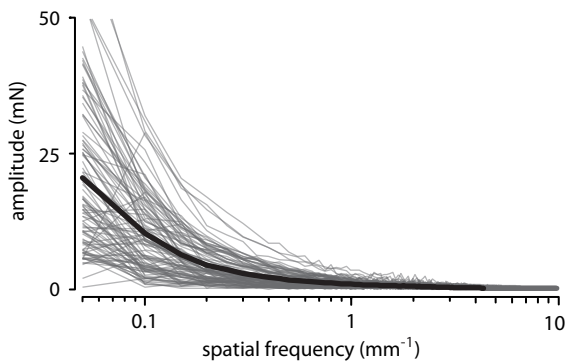


Figure 5: Individual measurements spectra (light gray) and average (black) of the measurement made with on the smooth flat surface.

The distribution of  $\alpha$  coefficients reaches a maximum at 0.9.

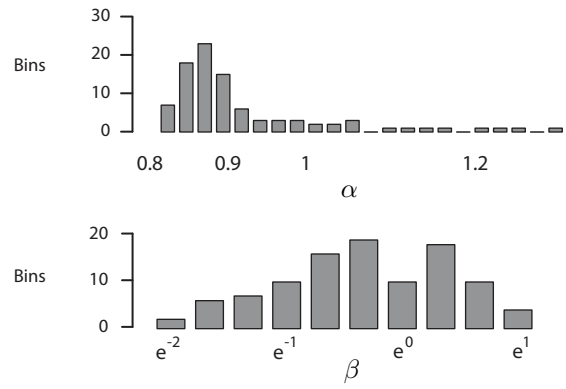


Figure 6: Distribution of fitted coefficients  $\alpha$  and  $\beta$  on the 100 measurements made with the smooth flat surface.

This feature indicates that the background noise is a fractal noise, found in numerous natural and man-made processes [14, 4]. The  $\beta$  value represents the magnitude of the fluctuations. This parameter is not related in any simple manner to any other parameter. The reader should keep in mind, however, that this noise behavior might be different for other materials than smooth epoxy.

The goodness of the fit for the power law is better than  $R^2 = 0.93$  for most cases. Fifteen outliers out of a hundred have a goodness of fit around 0.8 and in one case the fit has a value of 0.3.

### 4.3 Fundamental and Harmonic Amplitudes

As it might be expected, averaging the measurements made on the three gratings with same amplitude  $A = 25 \mu\text{m}$  but varying spatial frequencies shows that the fundamental peak of the force variations always coincided with spatial frequency of the original surface.

All harmonics are present in all three cases. Their decay can be well represented by a power-law function,  $S_h(k) = \beta_h/k^{\alpha_h}$ . Fitting the data shown in Fig. 7 gives estimates of the decay coefficient  $\alpha_h = \{1.5, 1.3, 1.3\}$  and magnitudes of  $\beta_h = \{e^{-2.2}, e^{-2.5}, e^{-2.3}\}$  for the spatial periods  $\lambda = \{1.76, 1.96, 2.5\} \text{ mm}$ , respectively.

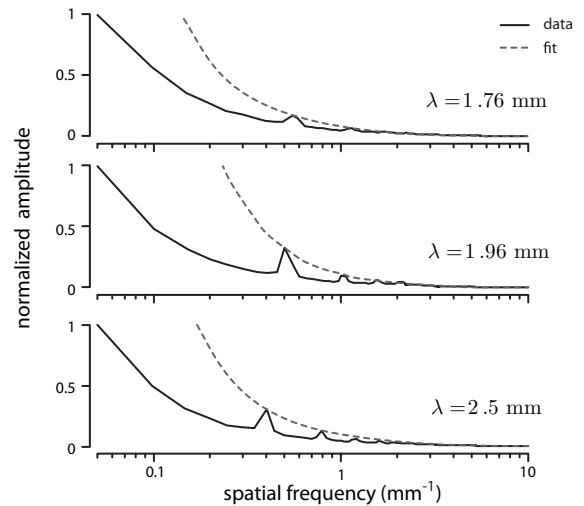


Figure 7: Spectrum average on the 3 spatial variations of the  $25 \mu\text{m}$  gratings in plain black. Power law fitting on the amplitude of fundamental and its harmonics is plotted in dashed grey.

#### 4.4 Influence of Grating Magnitude

The effect of the magnitudes of the gratings on the spatial spectra of the friction force fluctuations was studied with the three textures described earlier. Each grating was used to produce 100 measurements. The averaged results for all three gratings are plotted in Fig. 8.

The average spectra suggest that the magnitude of the surface undulation affects the amplitude of the fundamental component. The relationship is monotonic but probably not linear. Interestingly, however, the harmonic components do not seem to be affected by the gratings magnitude, at least within the range that we tested.

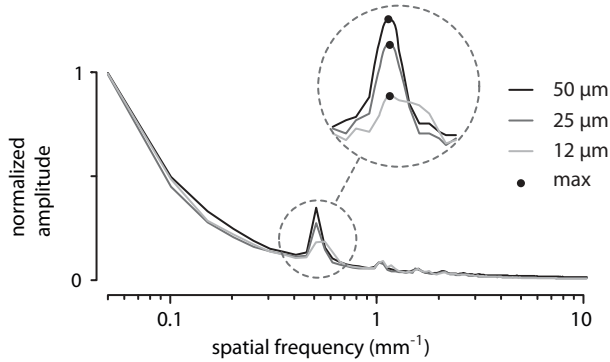


Figure 8: Spectrum averages of 100 measurements made with three gratings with same spatial period of 1.96 mm and variable amplitudes. Spectra were normalized relatively to their maxima in the low frequencies, below the frequency of the gratings.

### 5 DISCUSSION

The results presented above gives us a better understanding of the dynamic of the finger from a signal processing point of view and from the viewpoint of the mechanics involved.

#### 5.1 Background noise

The  $1/f$  background noise, present in the recordings, shine some light on the energy repartition of the vibration. This particular noise is found in many processes and has for particularity that the energy is constant in every decade band.

From a mechanical point of view, this trend can be explained by the fact that the height repartition of the smooth surface is close to white noise as its height density is a Gaussian function. By stroking our finger on the grating, this white noise drives a mechanical first order filter that represents a fingertip modeled by a spring and a dashpot.

It is worth noting that in signal generation, there is no simple way to spontaneously generate  $1/f$  noise. The common approach to synthesize this signal is achieved by filtering random white noise with a first order filter.

#### 5.2 Harmonic behavior

The fact that the harmonic behavior of force fluctuations is different from the background noise cannot be explained simply. The decay of the harmonics is non-integer which does not fit with viscous nor with inertial dynamics. One possible element of answer is that the finger impedance and the friction conditions are strongly non-linear, and therefore, the original sinusoidal forcing term becomes distorted and harmonics are created. The nonlinear transformation cannot simply be extrapolated from the measurements and requires analysis with more powerful tools such as Volterra series or Wiener kernels.

Another hypothesis can be formulated by supposing that the finger behaves like a distributed collection of oscillators forced by traction from the surface. Each of these oscillators undergoes stick-slip relaxation oscillations that are driven by the surface undulations. When one region of the skin sticks at one of the apices of the undulation, the skin is tangentially loaded, corresponding to a ramp in the interaction force. When the contact breaks away, energy is rapidly released corresponding to a cliff. The force waveform associated with one element will be close to sawtooth waveform. The later picture is consistent with an interaction force signal exhibiting a decay of all the harmonic amplitudes since the harmonics of a sawtooth signal have amplitudes that are inversely proportional to their number. The occurrence of these oscillations would be hidden in the temporal domain by the superposition of several out-of-phase oscillators. This enticing possibility merits further investigations.

#### 5.3 Energy dissipation

Van den Doel et al. proposed a scaling law for the ‘audio force’ based on the instantaneous motor power delivered when scanning a surface (i.e. the square root of the product of tangential force and velocity) [22]. They assumed that the mechanical energy spent during the exploration is dissipated by friction and entirely transferred into propagating vibrations. This assumption is valid for rigid probe friction on rough surface, however a bare finger may behave differently. Viscoelasticity and soft tissue friction generate vibrations, but when stroking a finger on a smooth unlubricated surface, an elevation of skin temperature can be felt. It is evident that some of the motoric work is transformed into heat.

For each trial, we estimated the work done by the participant to slide his finger and compared it to the vibratory signal energy. The motor work was calculated from  $W = \int_0^d F_t(x) dx$ , where  $d$  is the distance traveled,  $x$  is the net finger position and  $F_t$  is the tangential force component measured by the strain-gauge force sensor which is sensitive to DC and low frequencies components. The vibratory signal energy was determined from  $E_s = \int_0^D |f_T(t)|^2 dt$  where  $D$  is the duration of the movement,  $t$  is the time parameter and  $f_T(t)$  is the force signal from the piezoelectric transducer since it is sensitive to frequencies above 2.5 Hz.

Fig. 9 shows the relationship between the spent motor work and the signal energy for each trial. The linear regression with zero intercept of the vibration energy against motor work, shown in dashed grey, shows an acceptable fit with  $R^2 = 0.76$ . A first-order linear fit, shown in black, however, represents the data much better with  $R^2 = 0.88$ . The abscissa intercept is approximately at  $W_{min} = 2.5$  mJ. This measurement, alone, does not inform us on the proportion of energy spent on heat and on vibrations. It nevertheless suggests that the work of bare-finger friction is transferred

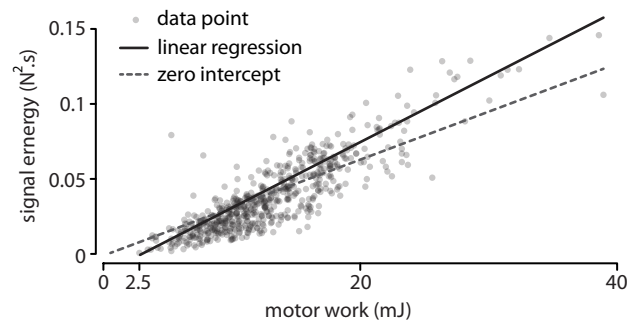


Figure 9: Relationship between the work spent during a recording and the corresponding measured force signal energy. Each dot represent one trial. The first-order fit represents the data better than the zero-order fit ( $R^2 = 0.88$  vs 0.76).

for the greatest part into vibrations originating at the finger-surface interface. The residual energy is dissipated into heat and probably radiated as sound waves.

The conditions that modify the surface-finger tribology are expected to greatly influence the proportions of the forms of dissipated energy, influencing in turn the information available for perceptual purposes. For instance, the vibrations arising from the frictional force can propagate in the surrounding air, giving acoustic cues, and in the skin giving tactile cues. Measurements of the finger and arm transmittance properties show that vibrations in the range 50 to 1000 Hz can travel as far as the forearm [8]. These results suggest that textures can possibly be sensed by very large populations of far flung mechanoreceptors located on the path of waves propagations.

## 6 CONCLUSION

We recorded accurate measurements of the force fluctuations generated by a finger exploring smooth flat and undulating surfaces. The spatial spectra of the signal shows that the vibrations are non deterministic but exhibit some interesting properties. With the smooth epoxy surface, we can characterize the background vibrations as a fractal noise with coefficient 0.9. The measurements with sinusoidal gratings reveal the nonlinearity of the skin interaction producing decaying harmonics compatible with the occurrence of a multiplicity of simultaneous relaxation oscillations.

These findings are the first steps toward the creation of virtual texture synthesis algorithms that are sensitive to various contact parameters and can generate appropriate vibrations. These findings can also possibly have perceptual implications since it can be proposed that the tactile system is sensitive to the peculiar dynamics involved. They also have possible contributions to make to the field of biotribology.

Future work will include finer experimentation on the influence of the material on the coefficient of the fractal noise, and its connection to the tribology and roughness. Moreover, other parameters such as the pose of the finger and hydration are likely to play dominant roles in the generation of tactual vibrations.

## ACKNOWLEDGEMENTS

The authors are grateful to A.M.L. Kappers for lending us the original gratings and Amir Berrezag for help on the casting procedure. They also would like to thank Yon Visell for his useful comments on the manuscript.

## REFERENCES

- [1] M. Adams, B. Briscoe, and S. Johnson. Friction and lubrication of human skin. *Tribology Letters*, 26(3):239–253, 2007.
- [2] T. Andre, P. Lefevre, and J. L. Thonnard. Fingertip moisture is optimally modulated during object manipulation. *Journal of Neurophysiology*, 103(1):402–408, 2010.
- [3] W. M. Bergmann-Tiest and A. M. L. Kappers. Analysis of haptic perception of materials by multidimensional scaling and physical measurements of roughness and compressibility. *Acta Psychologica*, 121(1):1–20, 2006.
- [4] V. Billock, G. de Guzman, and J. Scott Kelso. Fractal time and 1/f spectra in dynamic images and human vision. *Physica D: Nonlinear Phenomena*, 148(1-2):136–146, 2001.
- [5] G. Champion and V. Hayward. On the synthesis of haptic textures. *IEEE Transactions on Robotics*, 24(3):527–536, 2008.
- [6] G. Champion and V. Hayward. Fast calibration of haptic texture synthesis algorithms. *Haptics, IEEE Transactions on*, 2(2):85–93, 2009.
- [7] M. Costa and M. Cutkosky. Roughness perception of haptically displayed fractal surfaces. In *Proceedings of the ASME Dynamic Systems and Control Division*, volume 69, pages 1073–1079. Citeseer, 2000.
- [8] B. Delhayé, V. Hayward, P. Lefevre, and J. L. Thonnard. Textural vibrations in the forearm during tactile exploration. Poster 782.11 Annual Meeting of the Society for Neuroscience, 2010.

- [9] V. Guruswamy, J. Lang, and W. Lee. IIR Filter Models of Haptic Vibration Textures. *Instrumentation and Measurement, IEEE Transactions on*, 60(1):93–103, 2010.
- [10] M. Hollins, S. J. Bensmaïa, and S. Washburn. Vibrotactile adaptation impairs discrimination of fine, but not coarse, textures. *Somatosensory & motor research*, 18(4):253–262, 2001.
- [11] M. Hollins, R. Faldowski, S. Rao, and F. Young. Perceptual dimensions of tactile surface texture: A multidimensional scaling analysis. *Perception and Psychophysics*, 54(6):697–705, 1993.
- [12] R. Klatzky and S. Lederman. Tactile roughness perception with a rigid link interposed between skin and surface. *Perception and Psychophysics*, 61(4):591–607, 1999.
- [13] L. E. Krueger. Tactual perception in historical perspective: David Katz’s world of touch. In W. Schiff and E. Foulke, editors, *Tactual Perception; A Sourcebook*, pages 1–55. Cambridge University Press, 1982.
- [14] B. Mandelbrot. *The fractal geometry of nature*. Freeman, 1982.
- [15] H. Nefs, A. Kappers, and J. Koenderink. Amplitude and spatial-period discrimination in sinusoidal gratings by dynamic touch. *Perception*, 30(10):1263–1274, 2001.
- [16] T. C. Pataky, M. L. Latash, and V. M. Zatsiorsky. Viscoelastic response of the finger pad to incremental tangential displacements. *Journal of Biomechanics*, 38:1441–1449, 2005.
- [17] D. T. V. Pawluk and R. D. Howe. Dynamic lumped element response of the human fingerpad. *ASME Journal of Biomechanical Engineering*, 121:178–184, 1999.
- [18] B. N. J. Persson. Theory of rubber friction and contact mechanics. *Journal of Chemical Physics*, 15(8):3840–3861, 2001.
- [19] J. Siira and D. Pai. Haptic texturing—a stochastic approach. In *Robotics and Automation, 1996. Proceedings., 1996 IEEE International Conference on*, volume 1, pages 557–562. IEEE, 1996.
- [20] A. M. Smith, E. C. Chapman, M. Deslandes, J. S. Langlais, and M. P. Thibodeau. Role of friction and tangential force variation in the subjective scaling of tactile roughness. *Experimental Brain Research*, 144(2):211–223, 2002.
- [21] S. E. Tomlinson, R. Lewis, and J. M. Carré. Review of the frictional properties of finger-object contact when gripping. *Proceedings of the Institution of Mechanical Engineers; Part B; Journal of Engineering Tribology*, 221:841–850, 2007.
- [22] K. Van Den Doel, P. Kry, and D. Pai. FoleyAutomatic: physically-based sound effects for interactive simulation and animation. In *Proceedings of the 28th annual conference on Computer graphics and interactive techniques*, pages 537–544. ACM, 2001.
- [23] Q. Wang and V. Hayward. In vivo biomechanics of the fingerpad skin under local tangential traction. *Journal of Biomechanics*, 40(4):851–860, 2007.
- [24] P. H. Warman and A. R. Ennos. Fingerprints are unlikely to increase the friction of primate fingerpads. *The Journal of Experimental Biology*, 212:2016–2022, 2009.
- [25] M. Wiertelowski, J. Lozada, and V. Hayward. The spatial spectrum of tangential skin displacement can encode tactual texture. *IEEE Transactions on Robotics*, In press, 2011.
- [26] M. Wiertelowski, J. Lozada, E. Pissaloux, and V. Hayward. Causality inversion in the reproduction of roughness. In A. M. L. Kappers et al., editor, *Proceedings of Eurohaptics 2010*, volume 6192 of LNCS, pages 17–24. Springer-Verlag, 2010.